Journal of Materials Chemistry C

ROYAL SOCIETY OF CHEMISTRY

COMMUNICATION

View Article Online
View Journal | View Issue

Cite this: J. Mater. Chem. C, 2023, 11, 893

Received 14th November 2022,
Accepted 12th December 2022

DOI: 10.1039/d2tc04848e

rsc.li/materials-c

Amplification of dissymmetry factors by dihedral angle engineering in donor–acceptor type circularly polarized luminescence materials†

Xing-Yu Chen,[a] Ji-Kun Li,[a] Wen-Long Zhao,[b] Cheng-Zhuo Du,[a] Meng Li,[b] Chuan-Feng Chen[b] and Xiao-Ye Wang*[ac]

By employing aza[7]helicene as the chiral donor and triazine as the acceptor, we have developed a new type of circularly polarized luminescence material. The influence of the dihedral angle between the donor and acceptor moieties on the dissymmetry factors has been revealed for the first time, providing a novel strategy to amplify dissymmetry factors by engineering the dihedral angles in donor–acceptor type chiral materials.

Circularly polarized luminescence (CPL) materials have received broad attention during the past few decades[1–15] due to their potential applications in full-colour 3D displays,[16] biological detection,[17] encrypted data storage,[18] *etc.* In particular, various CPL materials have been developed for electroluminescent applications in circularly polarized organic light-emitting diodes (CP-OLEDs).[19–26] How to realize a high luminescence dissymmetry factor (g_{lum}), which characterizes the level of polarization and is defined by $g_{lum} = 2(I_L - I_R)/(I_L + I_R)$ (where I_L and I_R are the emission intensity of left-handed and right-handed circularly polarized light, respectively), has been the key challenge in the field to promote the practical applications of CPL materials.

On the other hand, to maximize the electroluminescence efficiency, thermally activated delayed fluorescence (TADF) materials, which can effectively convert triplet excitons into singlet excitons through reverse intersystem crossing (RISC) to achieve 100% internal quantum efficiency, have played a pivotal role in OLEDs.[27–29] Traditional TADF emitters usually consist of donor (D) and acceptor (A) moieties to furnish effective separation of the highest occupied molecular orbital (HOMO) and lowest unoccupied molecular orbital (LUMO), which can significantly reduce the energy gap between the singlet and triplet states (ΔE_{ST}) to boost RISC. Introducing chiral units into classical D–A type TADF materials is an effective strategy to construct emitters for CP-OLED applications.[30–42] Nevertheless, the g_{lum} values of D–A type CPL materials are generally low (in the range of 10^{-3} to 10^{-5}).[43–54] Besides, the lack of understanding of the impact of structural variations on the g_{lum} of D–A type CPL materials limits the rational improvement of g_{lum}.

Herein, we design a new type of CPL material by introducing aza[7]helicene[10] as the helical donor and triazine[28] as the acceptor, and for the first time, investigate the influence of the dihedral angle between the D–A parts on the g_{lum} of CPL materials (Fig. 1). Theoretical studies reveal a substantial dependence of g_{lum} on the dihedral angles. To further verify the structure–property correlations, we design and synthesize two CPL molecules with different dihedral angles by controlling the steric hindrance between the D–A units. A nearly two-fold amplification of g_{lum} is achieved experimentally, providing a

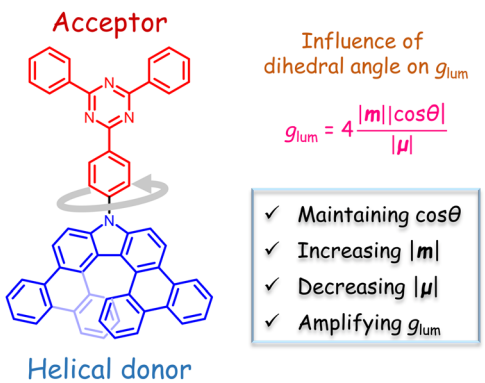

Fig. 1 Molecular design of new D–A type CPL materials in this work.

[a] State Key Laboratory of Elemento-Organic Chemistry, College of Chemistry, Nankai University, Tianjin 300071, China. E-mail: xiaoye.wang@nankai.edu.cn; Web: https://wang.nankai.edu.cn
[b] Beijing National Laboratory for Molecular Sciences, CAS Key Laboratory of Molecular Recognition and Function, Institute of Chemistry, Chinese Academy of Sciences, Beijing 100190, China
[c] State Key Laboratory of Luminescent Materials and Devices, South China University of Technology, Guangzhou 510640, China

† Electronic supplementary information (ESI) available: Synthetic procedures, characterization data, and theoretical calculations. See DOI: https://doi.org/10.1039/d2tc04848e

novel strategy to boost the g_{lum} of D–A type CPL materials by regulating the dihedral angle of the D–A moieties.

First, we introduced aza[7]helicene as the unprecedented chiral donor and 2,4,6-triphenyl-1,3,5-triazine as the acceptor to construct D–A type molecule **Trz-A7H** for theoretical investigations. Based on the optimized geometry of the singlet excited state (S_1), we varied the dihedral angle (C1–C2–N3–C4) to carry out a rigid scanning (Fig. 2). The impact of dihedral angles (from 45° to 135°) on the transition electric dipole moment ($\boldsymbol{\mu}$), the transition magnetic dipole moment ($\boldsymbol{m}$), and their angle θ was first studied because they jointly determine the g factor according to the calculation formula $g = 4|\cos\theta||\boldsymbol{m}|/|\boldsymbol{\mu}|$ ($|\boldsymbol{\mu}| \gg |\boldsymbol{m}|$) for common organic molecules (Fig. 2b).[11] It can be seen that with the increase of the dihedral angle, the $|\boldsymbol{\mu}|$ of **Trz-A7H** decreases first and then increases, resulting in a minimum value of 2.56×10^{-18} esu cm at 105°. Meanwhile, with the increase of the dihedral angle, the $|\boldsymbol{m}|$ of the molecule shows an opposite trend and reaches the maximum value of 0.70×10^{-20} erg G^{-1} at 100°. Besides, $|\cos\theta|$ does not change significantly and keeps close to 1 because $\boldsymbol{\mu}$ and $\boldsymbol{m}$ are aligned in parallel during the scanning of the dihedral angle. As a result, g_{lum} increases first and then decreases as the dihedral angle is raised, reaching 10.9×10^{-3} as the maximum value at 105° (Fig. 2c). Therefore, a more than two-fold amplification of g_{lum} can be expected in theory by engineering the dihedral angle of the D–A type CPL materials.

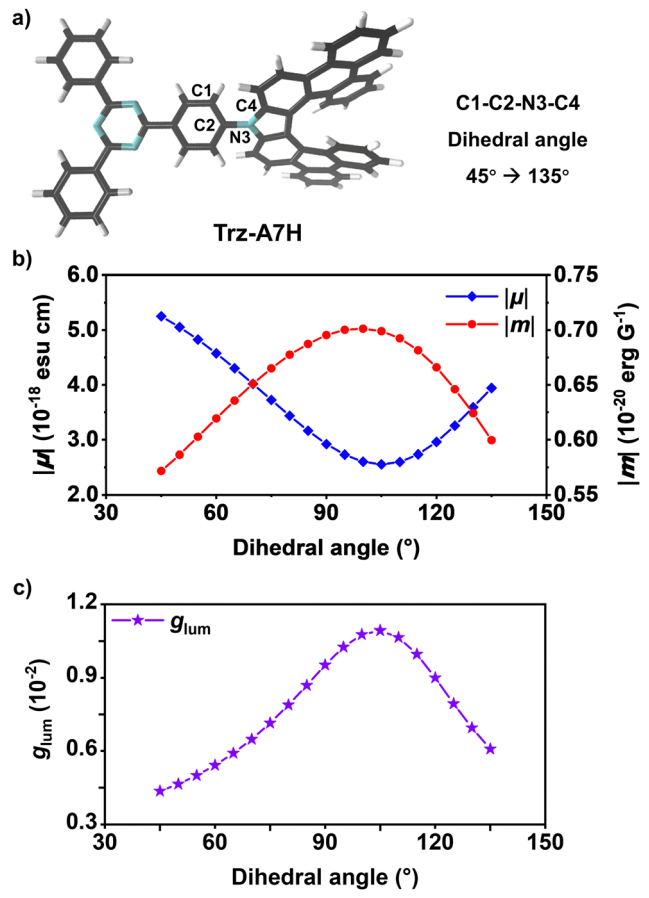

Fig. 2 (a) The structure model of **Trz-A7H** investigated in this work and the illustration of the dihedral angle between the donor and acceptor units. (b) $|\mu|$ and $|m|$ as a function of the dihedral angle. (c) g_{lum} as a function of the dihedral angle.

Based on the theoretical results, we synthesized two molecules (**Trz-A7H** and **DMTrz-A7H**) for experimental verification of the g_{lum} amplification strategy (Scheme 1). The dihedral angle between the donor and acceptor moieties is regulated by introducing two methyl groups *ortho* to the aza[7]helicene substituent to increase the steric hindrance. Density functional theory (DFT) calculations show that the introduction of methyl groups increases the dihedral angle between the donor and acceptor parts from 54° (**Trz-A7H**) to 92° (**DMTrz-A7H**) in the ground state (S_0), and from 47° to 74° in the S_1 state. The synthetic routes to **Trz-A7H** and **DMTrz-A7H** are depicted in Scheme 1. The aza[7]helicene derivative (**3**) was first synthesized according to the reported procedure.[10] Then **Trz-A7H** and **DMTrz-A7H** were obtained through aromatic nucleophilic substitution reactions of 2-(4-fluorophenyl)-4,6-diphenyl-1,3,5-triazine (**1**) and 2-(4-fluoro-3,5-dimethylphenyl)-4,6-diphenyl-1,3,5-triazine (**2**) with **3** in 30% and 26% yields, respectively. Their structures were confirmed by ^{1}H and ^{13}C NMR spectroscopies and high-resolution mass spectrometry.

UV-vis absorption spectra show that **Trz-A7H** and **DMTrz-A7H** have very similar optical properties (Fig. 3a). The lowest-energy absorption maximum of **DMTrz-A7H** is at 417 nm ($\varepsilon = 1.16 \times 10^4$ M^{-1} cm^{-1}), which is slightly blue-shifted compared with **Trz-A7H** (420 nm, $\varepsilon = 1.33 \times 10^4$ M^{-1} cm^{-1}). Both **DMTrz-A7H** and **Trz-A7H** exhibit blue emission peaking at 426 nm and 431 nm, respectively (Fig. 3b). These results imply that the change of dihedral angle has only a negligible effect on the photophysical properties of the two molecules. Based on the electrochemical characterizations, the HOMO/LUMO energy levels of **DMTrz-A7H** and **Trz-A7H** are −5.61/−2.79 eV and −5.59/−2.77 eV, respectively (Fig. S7, ESI†). The electrochemical gaps are both 2.82 eV for **DMTrz-A7H** and **Trz-A7H**,

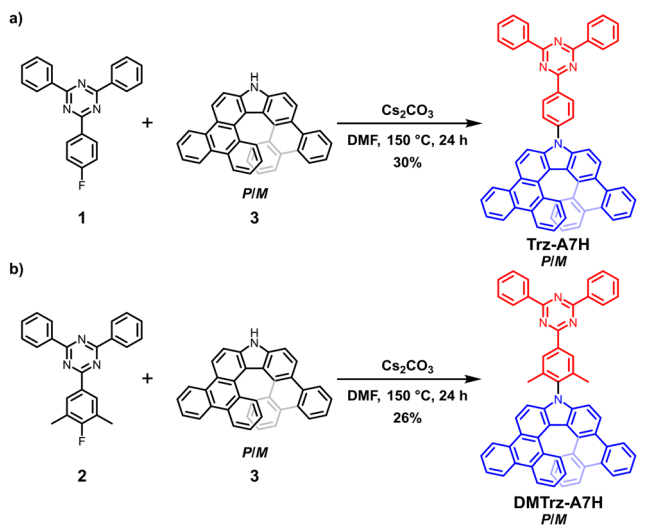

Scheme 1 Synthetic routes to (a) **Trz-A7H** and (b) **DMTrz-A7H**.

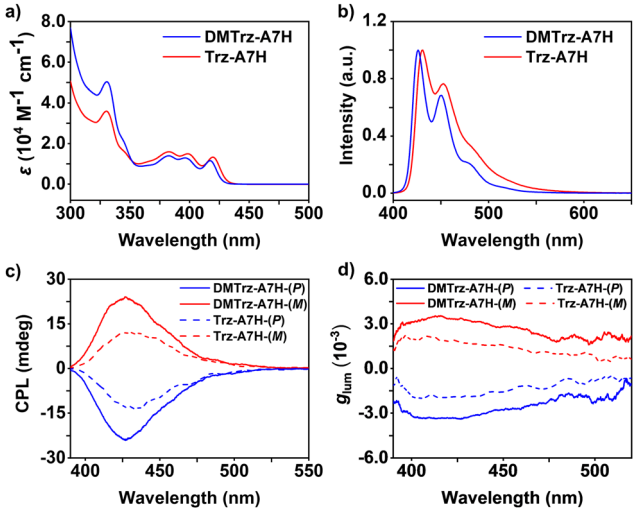

Fig. 3 (a) UV-vis absorption and (b) emission spectra of **Trz-A7H** and **DMTrz-A7H** in toluene (c = 1 × 10^{-5} M). (c) CPL spectra and (d) g_{lum} of **Trz-A7H** and **DMTrz-A7H** in toluene (c = 1 × 10^{-5} M).

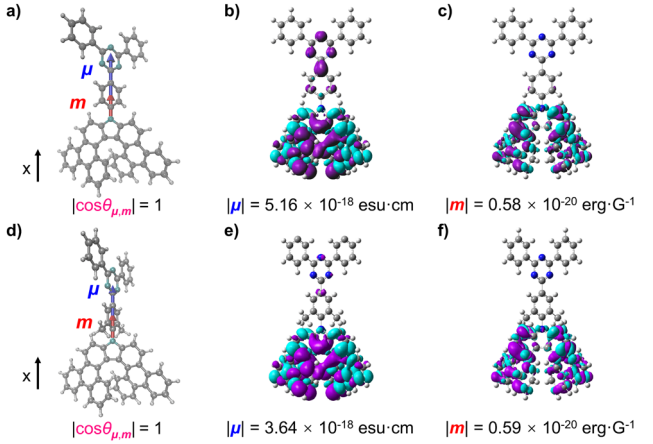

Fig. 4 Transition electric and magnetic dipole moments of (a) **Trz-A7H** and (d) **DMTrz-A7H**, where the length of the transition magnetic dipole moment vector is multiplied by 120 for clarity. The transition electric dipole moment density (only for the x axis component) of (b) **Trz-A7H** and (e) **DMTrz-A7H**. The transition magnetic dipole moment density (only for x axis component) of (c) **Trz-A7H** and (f) **DMTrz-A7H**. Both transition electric and magnetic dipole moment densities are calculated for the $S_1 \rightarrow S_0$ transition displayed with an iso-surface value of 0.002 a.u.

which is consistent with their optical gaps (2.89 eV and 2.87 eV, respectively). The photoluminescence quantum yield (PLQY) of **DMTrz-A7H** in degassed toluene is 43%, which is slightly lower than that of **Trz-A7H** (55%).

Chiral separation of **DMTrz-A7H** and **Trz-A7H** was successfully achieved through high-performance liquid chromatography (HPLC) by using the Daicel Chiralpak IE column, thanks to their high configurational stability as revealed by transition-state calculations (Fig. S8 and S9, ESI†). The chiroptical properties of **DMTrz-A7H** and **Trz-A7H** were thus characterized. Each pair of enantiomers (**DMTrz-A7H** and **Trz-A7H**) has circular dichroism (CD) responses ranging from 280 to 450 nm with opposite Condon effects (Fig. S5, ESI†). The configuration of *P* and *M* was confirmed by comparing the experimental CD spectra with the simulated result (Fig. S11, ESI†). The absolute absorption dissymmetry factors ($|g_{abs}|$) of **DMTrz-A7H** and **Trz-A7H** are plotted as a function of wavelength according to the equation $|g_{abs}| = |\Delta\varepsilon|/\varepsilon$. The $|g_{abs}|$ of **DMTrz-A7H** is significantly larger than that of **Trz-A7H** beyond 400 nm (S_0 to S_1 transition), indicating that the $|g_{abs}|$ can be increased by changing the dihedral angle of D–A type molecules in the ground state. Meanwhile, **DMTrz-A7H** and **Trz-A7H** show similar CPL responses between 390 nm and 500 nm, which are assigned to the transition from S_1 to S_0. The strongest CPL response of **DMTrz-A7H** (427 nm, 24 mdeg) is about twice that of **Trz-A7H** (427 nm, 12 mdeg) at the same concentration (Fig. 3c). Moreover, the maximum $|g_{lum}|$ of **DMTrz-A7H** (3.5 × 10^{-3}) is also about twice that of **Trz-A7H** (2.1 × 10^{-3}), which is basically consistent with the theoretical results (Fig. 3d).

In order to further understand why g_{lum} of **DMTrz-A7H** is higher than that of **Trz-A7H** after changing the dihedral angle between the donor and acceptor units, the vector and density distributions of $\boldsymbol{m}$ and $\boldsymbol{\mu}$ of **DMTrz-A7H** and **Trz-A7H** were calculated.[55,56] The calculation results show that the $\boldsymbol{m}$ and $\boldsymbol{\mu}$ directions of both compounds are the same, so that $\cos\theta$ is kept at the maximum value of 1, which indicates the negligible effect on $\cos\theta$ by changing the dihedral angle (Fig. 4a and d). The transition magnetic dipole moment densities of positive (purple) and negative (blue) transitions are completely distributed on the donor part, indicating their absolute contributions to $\boldsymbol{m}$, with 0.59 × 10^{-20} erg G^{-1} for **DMTrz-A7H** and 0.58 × 10^{-20} erg G^{-1} for **Trz-A7H**, respectively (Fig. 4c and f). Meanwhile, the transition electric dipole moment density of the two molecules (Fig. 4b and e) has a similar distribution on the donor moiety, but some positive (purple) contributions are distributed on the triazine core in **Trz-A7H**, but not in **DMTrz-A7H**, leading to the smaller $|\boldsymbol{\mu}|$ of **DMTrz-A7H** (3.64 × 10^{-18} esu cm) than that of **Trz-A7H** (5.16 × 10^{-18} esu cm). According to the formula $g = 4|\cos\theta||\boldsymbol{m}|/|\boldsymbol{\mu}|$, these results suggest that the main reason why $|g_{lum}|$ of **DMTrz-A7H** is higher than that of **Trz-A7H** is the decrease of $|\boldsymbol{\mu}|$ due to the increase of the dihedral angle between the donor and acceptor, which is consistent with the trend of $|\boldsymbol{\mu}|$ obtained by theoretical calculations.

In summary, we have disclosed the effect of dihedral angles on g_{lum} in D–A type CPL materials for the first time through theoretical simulation and experimental verification. We have introduced aza[7]helicene as the unprecedented helical donor and 2,4,6-triphenyl-1,3,5-triazine as the acceptor to develop new D–A type CPL molecules. Theoretical calculations have revealed that g_{lum} is highly dependent on the dihedral angles, reaching a maximum value at an ideal angle. Experimentally modulating the dihedral angle has been achieved by introducing additional methyl groups to **Trz-A7H**, and a nearly two-fold amplification of g_{lum} has been demonstrated. This work thus provides a novel strategy to boost the g_{lum} of D–A type CPL materials by modulating the dihedral angles. In light of the vital role of D–A molecules in TADF OLEDs, this work will further promote

the development of high-performance CPL materials for CP-OLED applications.

Conflicts of interest

There are no conflicts to declare.

Acknowledgements

We are grateful for the financial support from the National Natural Science Foundation of China (No. 21901128, 22071120 and 92256304), the National Key R&D Program of China (2020YFA0711500), the Open Fund of the State Key Laboratory of Luminescent Materials and Devices (South China University of Technology), and the Fundamental Research Funds for the Central Universities.

Notes and references

1 Z. Qiu, C.-W. Ju, L. Frédéric, Y. Hu, D. Schollmeyer, G. Pieters, K. Müllen and A. Narita, *J. Am. Chem. Soc.*, 2021, **143**, 4661–4667.
2 Q. Meng, L. Cui, Q. Liao, J. Xu and Y. Wang, *Chem. Commun.*, 2022, **58**, 10384–10387.
3 J. Liu, L. Jiang, H. Chang, H. Liu, X.-Y. Cao, Y. Zou and Y. Hu, *Chem. Commun.*, 2022, **58**, 13087–13090.
4 A. Garci, S. Abid, A. H. G. David, M. D. Codesal, L. Đorđević, R. M. Young, H. Sai, L. Le Bras, A. Perrier, M. Ovalle, P. J. Brown, C. L. Stern, A. G. Campaña, S. I. Stupp, M. R. Wasielewski, V. Blanco and J. F. Stoddart, *Angew. Chem., Int. Ed.*, 2022, **61**, e202208679.
5 S. Garain, S. Sarkar, B. Chandra Garain, S. K. Pati and S. J. George, *Angew. Chem., Int. Ed.*, 2022, **61**, e202115773.
6 B. C. Baciu, P. J. Bronk, T. de Ara, R. Rodriguez, P. Morgante, N. Vanthuyne, C. Sabater, C. Untiedt, J. Autschbach, J. Crassous and A. Guijarro, *J. Mater. Chem. C*, 2022, **10**, 14306–14318.
7 Z. Zhang, T. Harada, A. Pietropaolo, Y. Wang, Y. Wang, X. Hu, X. He, H. Chen, Z. Song, M. Bando and T. Nakano, *Chem. Commun.*, 2021, **57**, 1794–1797.
8 Y. Ru, L. Sui, H. Song, X. Liu, Z. Tang, S.-Q. Zang, B. Yang and S. Lu, *Angew. Chem., Int. Ed.*, 2021, **60**, 14091–14099.
9 W. J. Li, Q. Gu, X. Q. Wang, D. Y. Zhang, Y. T. Wang, X. He, W. Wang and H. B. Yang, *Angew. Chem., Int. Ed.*, 2021, **60**, 9507–9515.
10 C. Maeda, K. Nagahata, T. Shirakawa and T. Ema, *Angew. Chem., Int. Ed.*, 2020, **59**, 7813–7817.
11 T. Mori, *Chem. Rev.*, 2021, **121**, 2373–2412.
12 D.-W. Zhang, M. Li and C.-F. Chen, *Chem. Soc. Rev.*, 2020, **49**, 1331–1343.
13 H. Tanaka, M. Ikenosako, Y. Kato, M. Fujiki, Y. Inoue and T. Mori, *Commun. Chem.*, 2018, **1**, 38.
14 H. Tanaka, Y. Inoue and T. Mori, *ChemPhotoChem*, 2018, **2**, 386–402.
15 J.-K. Li, X.-Y. Chen, Y.-L. Guo, X.-C. Wang, A. C.-H. Sue, X.-Y. Cao and X.-Y. Wang, *J. Am. Chem. Soc.*, 2021, **143**, 17958–17963.
16 H. Feng, Q. Li, W. Wan, J.-H. Song, Q. Gong, M. L. Brongersma and Y. Li, *ACS Photonics*, 2019, **6**, 2910–2916.
17 N. Nishizawa, A. Hamada, K. Takahashi, T. Kuchimaru and H. Munekata, *Jpn. J. Appl. Phys.*, 2020, **59**, SEEG03.
18 Y.-A. Chen, Q. Zhang, T.-Y. Chen, W.-Q. Cai, S.-K. Liao, J. Zhang, K. Chen, J. Yin, J.-G. Ren, Z. Chen, S.-L. Han, Q. Yu, K. Liang, F. Zhou, X. Yuan, M.-S. Zhao, T.-Y. Wang, X. Jiang, L. Zhang, W.-Y. Liu, Y. Li, Q. Shen, Y. Cao, C.-Y. Lu, R. Shu, J.-Y. Wang, L. Li, N.-L. Liu, F. Xu, X.-B. Wang, C.-Z. Peng and J.-W. Pan, *Nature*, 2021, **589**, 214–219.
19 H. Yan, J. Wade, L. Wan, S. Kwon, M. J. Fuchter, A. J. Campbell and J.-S. Kim, *J. Mater. Chem. C*, 2022, **10**, 9512–9520.
20 L. Wan, J. Wade, X. Wang, A. J. Campbell and M. J. Fuchter, *J. Mater. Chem. C*, 2022, **10**, 5168–5172.
21 K. Dhbaibi, L. Abella, S. Meunier-Della-Gatta, T. Roisnel, N. Vanthuyne, B. Jamoussi, G. Pieters, B. Racine, E. Quesnel, J. Autschbach, J. Crassous and L. Favereau, *Chem. Sci.*, 2021, **12**, 5522–5533.
22 J. Cheng, F. Ge, Y. Xiang, H. Zhang, Y. Kuai, P. Hou, D. Zhang, L. Qiu, Q. Zhang and G. Zou, *J. Mater. Chem. C*, 2020, **8**, 6521–6527.
23 Z.-G. Wu, Z.-P. Yan, X.-F. Luo, L. Yuan, W.-Q. Liang, Y. Wang, Y.-X. Zheng, J.-L. Zuo and Y. Pan, *J. Mater. Chem. C*, 2019, **7**, 7045–7052.
24 G. Fu, Y. He, W. Li, B. Wang, X. Lü, H. He and W.-Y. Wong, *J. Mater. Chem. C*, 2019, **7**, 13743–13747.
25 E. Peeters, M. P. T. Christiaans, R. A. J. Janssen, H. F. M. Schoo, H. P. J. M. Dekkers and E. W. Meijer, *J. Am. Chem. Soc.*, 1997, **119**, 9909–9910.
26 L. Zhou, G. Xie, F. Ni and C. Yang, *Appl. Phys. Lett.*, 2020, **117**, 130502.
27 H. Uoyama, K. Goushi, K. Shizu, H. Nomura and C. Adachi, *Nature*, 2012, **492**, 234–238.
28 L.-S. Cui, H. Nomura, Y. Geng, J. U. Kim, H. Nakanotani and C. Adachi, *Angew. Chem., Int. Ed.*, 2017, **56**, 1571–1575.
29 Z. Yang, Z. Mao, Z. Xie, Y. Zhang, S. Liu, J. Zhao, J. Xu, Z. Chi and M. P. Aldred, *Chem. Soc. Rev.*, 2017, **46**, 915–1016.
30 L. Zhou, F. Ni, N. Li, K. Wang, G. Xie and C. Yang, *Angew. Chem., Int. Ed.*, 2022, **61**, e202203844.
31 S.-Y. Yang, Q.-S. Tian, X.-J. Liao, Z.-G. Wu, W.-S. Shen, Y.-J. Yu, Z.-Q. Feng, Y.-X. Zheng, Z.-Q. Jiang and L.-S. Liao, *J. Mater. Chem. C*, 2022, **10**, 4393–4401.
32 Y.-F. Wang, X. Liu, Y. Zhu, M. Li and C.-F. Chen, *J. Mater. Chem. C*, 2022, **10**, 4805–4812.
33 J.-M. Teng, D.-W. Zhang, Y.-F. Wang and C.-F. Chen, *ACS Appl. Mater. Interfaces*, 2022, **14**, 1578–1586.
34 M. Li and C.-F. Chen, *Chem. – Eur. J.*, 2022, **28**, e202103550.
35 J. M. dos Santos, D. Sun, J. M. Moreno-Naranjo, D. Hall, F. Zinna, S. T. J. Ryan, W. Shi, T. Matulaitis, D. B. Cordes, A. M. Z. Slawin, D. Beljonne, S. L. Warriner, Y. Olivier, M. J. Fuchter and E. Zysman-Colman, *J. Mater. Chem. C*, 2022, **10**, 4861–4870.
36 Z. Chen, C. Zhong, J. Han, J. Miao, Y. Qi, Y. Zou, G. Xie, S. Gong and C. Yang, *Adv. Mater.*, 2022, **34**, e2109147.
37 Y.-P. Zhang, X. Liang, X.-F. Luo, S.-Q. Song, S. Li, Y. Wang, Z.-P. Mao, W.-Y. Xu, Y.-X. Zheng, J.-L. Zuo and Y. Pan, *Angew. Chem., Int. Ed.*, 2021, **60**, 8435–8440.

38 D.-W. Zhang, J.-M. Teng, Y.-F. Wang, X.-N. Han, M. Li and C.-F. Chen, *Mater. Horiz.*, 2021, **8**, 3417–3423.
39 Y. Xu, Q. Wang, X. Cai, C. Li and Y. Wang, *Adv. Mater.*, 2021, **33**, e2100652.
40 Y.-F. Wang, M. Li, J.-M. Teng, H.-Y. Zhou, W.-L. Zhao and C.-F. Chen, *Angew. Chem., Int. Ed.*, 2021, **60**, 23619–23624.
41 Z.-L. Tu, J.-J. Lu, X.-F. Luo, J.-J. Hu, S. Li, Y. Wang, Y.-X. Zheng, J.-L. Zuo and Y. Pan, *Adv. Opt. Mater.*, 2021, **9**, 2100596.
42 P. Sumsalee, L. Abella, S. Kasemthaveechok, N. Vanthuyne, M. Cordier, G. Pieters, J. Autschbach, J. Crassous and L. Favereau, *Chem. – Eur. J.*, 2021, **27**, 16505–16511.
43 T.-T. Liu, Z.-P. Yan, J.-J. Hu, L. Yuan, X.-F. Luo, Z.-L. Tu and Y.-X. Zheng, *ACS Appl. Mater. Interfaces*, 2021, **13**, 56413–56419.
44 L. Frédéric, A. Desmarchelier, L. Favereau and G. Pieters, *Adv. Funct. Mater.*, 2021, **31**, 2010281.
45 S.-Y. Yang, Y.-K. Wang, C.-C. Peng, Z.-G. Wu, S. Yuan, Y.-J. Yu, H. Li, T.-T. Wang, H.-C. Li, Y.-X. Zheng, Z.-Q. Jiang and L.-S. Liao, *J. Am. Chem. Soc.*, 2020, **142**, 17756–17765.
46 Y. Wang, Y. Zhang, W. Hu, Y. Quan, Y. Li and Y. Cheng, *ACS Appl. Mater. Interfaces*, 2019, **11**, 26165–26173.
47 S. Feuillastre, M. Pauton, L. Gao, A. Desmarchelier, A. J. Riives, D. Prim, D. Tondelier, B. Geffroy, G. Muller, G. Clavier and G. Pieters, *J. Am. Chem. Soc.*, 2016, **138**, 3990–3993.
48 L. Frédéric, A. Desmarchelier, R. Plais, L. Lavnevich, G. Muller, C. Villafuerte, G. Clavier, E. Quesnel, B. Racine, S. Meunier-Della-Gatta, J. P. Dognon, P. Thuéry, J. Crassous, L. Favereau and G. Pieters, *Adv. Funct. Mater.*, 2020, **30**, 2004838.
49 Z.-G. Wu, H.-B. Han, Z.-P. Yan, X.-F. Luo, Y. Wang, Y.-X. Zheng, J.-L. Zuo and Y. Pan, *Adv. Mater.*, 2019, **31**, 1900524.
50 Z.-L. Tu, Z.-P. Yan, X. Liang, L. Chen, Z.-G. Wu, Y. Wang, Y.-X. Zheng, J.-L. Zuo and Y. Pan, *Adv. Sci.*, 2020, **7**, 2000804.
51 F. Song, Z. Xu, Q. Zhang, Z. Zhao, H. Zhang, W. Zhao, Z. Qiu, C. Qi, H. Zhang, H. H. Y. Sung, I. D. Williams, J. W. Y. Lam, Z. Zhao, A. Qin, D. Ma and B.-Z. Tang, *Adv. Funct. Mater.*, 2018, **28**, 1800051.
52 M. Li, S.-H. Li, D. Zhang, M. Cai, L. Duan, M.-K. Fung and C.-F. Chen, *Angew. Chem., Int. Ed.*, 2018, **57**, 2889–2893.
53 M. Li, Y. Liu, R. Duan, X. Wei, Y. Yi, Y. Wang and C. F. Chen, *Angew. Chem., Int. Ed.*, 2017, **56**, 8818–8822.
54 M. Li, Y.-F. Wang, D. Zhang, L. Duan and C.-F. Chen, *Angew. Chem., Int. Ed.*, 2020, **59**, 3500–3504.
55 H. Kubo, T. Hirose, T. Nakashima, T. Kawai, J. Y. Hasegawa and K. Matsuda, *J. Phys. Chem. Lett.*, 2021, **12**, 686–695.
56 T. Lu and F. Chen, *J. Comput. Chem.*, 2012, **33**, 580–592.